Pharm Res (2015) 32:3376–3390
DOI 10.1007/s11095-015-1714-2

RESEARCH PAPER

Glycyrrhetinic Acid-Mediated Polymeric Drug Delivery Targeting the Acidic Microenvironment of Hepatocellular Carcinoma

Jinming Zhang[1] • Min Zhang[2] • Juan Ji[3] • Xiefan Fang[4] • Xin Pan[3] • Yitao Wang[1] • Chuanbin Wu[3] • Meiwan Chen[1]

Received: 26 February 2015 / Accepted: 14 May 2015 / Published online: 7 July 2015

ABSTRACT

Purpose The major hurdle of current drug carrier against hepatocellular carcinoma (HCC) is the lack of specific and selective drug delivery to HCC. In this study, a novel glycyrrhetinic acid (GA) and poly(L-Histidine) (PHIS) mediated polymeric drug delivery system was developed to target HCC that have GA binding receptors and release its encapsulated anticancer drug in the acidic microenvironment of HCC.

Methods Firstly, GA and PHIS were conjugated to form poly (ethylene glycol)-poly(lactic-co-glycolic acid) (GA-PEG-PHIS-PLGA, GA-PPP) micelles by grafting reaction between active terminal groups. Secondly, andrographolide (AGP) was encapsulated to GA-PPP to make AGP/GA-PPP using the solvent evaporation method. The pH-responsive property of AGP/GA-PPP micelles was validated by monitoring its stability and drug release behavior in different pH conditions. Furthermore, selective hepatocellular uptake of GA-PPP micelles *in vitro*, liver specific drug accumulation *in vivo,* as well as the enhanced antitumor effects of AGP/GA-PPP micelles confirmed the HCC targeting property of our novel drug delivery system.

Results Average size of AGP/GA-PPP micelles increased significantly and the encapsulated AGP released faster *in vitro* at pH 5.0, while micelles keeping stable in pH 7.4. AGP/GA-PPP micelles were uptaken more efficiently by human Hep3B liver cells than that by human MDA-MB-231 breast cancer cells. GA-PPP micelles accumulated specifically in the liver and possessed long retention time *in vivo*. AGP/GA-PPP micelles significantly inhibited tumor growth and provided better therapeutic outcomes compared to free AGP and AGP/PEG-PLGA(AGP/PP) micelles without GA and PHIS decoration.

Conclusions This novel GA-PPP polymeric carrier is promising for targeted treatment of HCC.

KEY WORDS andrographolide · hepatocellular carcinoma · glycyrrhetinic acid · micelles · pH-sensitive

ABBREVIATIONS

AFM	Atomic force microscopy
AGP	Andrographolide
ANOVA	Analysis of variance
6-C/GA-PPP	6-C loaded GA-PPP micelles
CLSM	Confocal laser scanning microscopy
DCC	N, N'-Dicyclohexylcarbodiimide
DCU	N, N'-Dicyclohexylurea
DMEM	Dulbecco's modified eagle medium

Electronic supplementary material The online version of this article (doi:10.1007/s11095-015-1714-2) contains supplementary material, which is available to authorized users.

✉ Yitao Wang
ytwang@umac.mo

✉ Meiwan Chen
mwchen@umac.mo

[1] State Key Laboratory of Quality Research in Chinese Medicine, Institute of Chinese Medical Sciences, University of Macau, Av. Padre Tomas Pereira S.J., Taipa, Macau 999078, China

[2] School of Chemistry and Chemical engineering, South China University of Technology, Guangzhou 510640, China

[3] School of Pharmaceutical Sciences, Sun Yat-sen University, Guangzhou 510006, China

[4] Department of Pediatrics, College of Medicine, University of Florida, Gainesville, FL 32610, USA

EPR	Enhanced permeability and retention
FBS	Fetal bovine serum
FTIR	Fourier transform infrared spectroscopy
GA	Glycyrrhetinic acid
GA-PEG-NH2	GA coupled-poly(ethylene glycol) with NH2 terminal
GA-PPP	GA-PEG-PHIS-PLGA
HCC	Hepatocellular carcinoma
H&E	Haematoxylin/eosin
ICG	Indocyanine green
MTT	3-(4,5-Dimethylthiazol-2-yl)-2,5-diphenyl tetrazolium bromide
NHS	N-hydroxysuccinimide
NMR	Nuclear magnetic resonance
PHIS	Poly(L-histidine)
PI	Propidium iodide
PLGA-PHIS	Poly(lactic-co-glycolic acid)-block-poly (L-histidine)
PP	PEG-PLGA

INTRODUCTION

Hepatocellular carcinoma (HCC) is one of the most common liver cancers and is the third leading cause for mortality among malignant neoplasms (1). Currently, only a small number of chemotherapeutic agents were developed to specifically target HCC cells, which had abundant endoplasmic reticulum (2). But these chemotherapeutic agents distribute systematically, leading to low tumor targeting and toxicity. Therefore, it is very important to develop novel drug delivery system to selectively target HCC. In recent decades, polymeric micelles have been proved to have high biosafety and drug loading efficiency, long retention time in blood circulation, as well as enhanced permeability and retention (EPR) effects (3). It is feasible to use polymeric micelles as vehicles to selectively deliver chemotherapeutic agents to cancer cells (4). However, no effective nano-micelles therapy has been developed so far to selectively target HCC (5, 6).

Glycyrrhetinic acid (GA), a natural occurring compound isolated from licorice (7), has been demonstrated to possess abundant receptors with high binding affinity on cellular membrane of hepatocytes (8). The targeting binding site of GA was identified as protein kinase C, which is expressed more highly in HCC cells than in the adjacent non-tumor live cells. There is significant interest in the use of GA as a ligand to functionalize HCC-targeting drug carriers such as nanospheres (9, 10), liposomes (11), and micelles (12) to improve the anti-HCC properties. These GA modified NPs exhibited more efficient liver- or hepatocyte-targeted capacity than non-GA-modified NPs (13, 14). Most importantly, GA ligands could escape shortages of some current ligands such as insufficient specificity of asialoglycoprotein receptor (15) and immune reactions caused by monoclonal antibodies and growth factor-recognizing oligopeptides (16).

Furthermore, the gradual drug release profiles of drugs from micelles are also another important obstacle for satisfactory clinical outcome (17). The pH-responsive strategy in polymers has been widely used for controlled intracellular drug release in recent years (18–22). This approach keeps drug release from micelles steady in normal pH condition due to the slow hydrolytic degradation of polyesters, and it accelerates drug release in acidic microenvironment presented in HCC tissues (23). Therefore, pH-sensitive NPs remain stable in physiological environment (pH≈7.4), but suffer fast disintegration in endosome or lysosome at pH 5 ~ 7 (24). Poly(L-histidine) (PHIS) has been demonstrated as an excellent candidate polymer for pH-sensitive drug release because of protonation of its imidazole groups in acidic cytoplasm (pH < 6.5) and its ability to escape from endosome.

To the best of our knowledge, it has not been reported to utilize liver targeting by GA ligand and pH-triggered drug release polymers to achieve dual-functional drug delivery systems. In the present study, we developed a novel polymeric drug delivery system, *i.e.*, glycyrrhetinic acid (GA) and poly(L-Histidine) conjugated with poly(ethylene glycol)-poly(lactic-co-glycolic acid) (GA-PEG-PHIS-PLGA, GA-PPP), by the solvent evaporation method. A model anticancer drug, andrographolide (AGP), was encapsulated to form AGP/GA-PPP micelles, which specifically targeted HCC by GA-binding hepatocyte receptors and released AGP under the acidic environment of HCC.

MATERIALS AND METHODS

Materials

18α-Glycyrrhetinic acid (GA, purity >98% by HPLC) and andrographolide (AGP, purity >98% by HPLC) were purchased from Jinzhu Pharmaceutical Co., Ltd. (Nanjing, China). PEG-$(NH_2)_2$ (MW = 5000) was supplied by Xibao Biotechnology Co., Ltd. (Shanghai, China). Poly (L-histidine) (MW = 5000 ~ 25000) was purchased from Sigma-Aldrich (St. Louis, MO, USA). Carboxyl-terminated PLGA polymer (MW = 5000, IV(dl/g) = 0.08) and mPEG-PLGA copolymer (PP, MW = 5000 for both PEG and PLGA polymers), which is a nonfunctional copolymer control were purchased from Daigang Biomaterial Co., Ltd (Jinan, China). N, N'-Dicyclohexylcarbodiimide (DCC) and N-hydroxysuccinimide (NHS) were obtained from GL Biochem., Ltd. (Shanghai, China). Coumarin 6 (laser grade) and ICG (free of sodium iodide) were used as fluorescence labels, obtained from Aladdin Reagent Co., Ltd (Shanghai, China).

For cell culture experiments, human Hep3B liver cancer cells and human MDA-MB-231 breast cancer cells were obtained from ATCC (Manassas, USA). 3-(4,5-Dimethylthiazol-2-yl)-2,5-diphenyl tetrazolium bromide (MTT), Dulbecco's Modified Eagle Medium (DMEM), and fetal bovine serum (FBS) were purchased from Sigma-Aldrich.

BALB/c nude mice (18 ~ 22 g) were obtained from the Animal Care Center at Sun Yat-Sen University. Animal experiments were performed according to the Guiding Principles for the Care and Use of Experiment Animals at Sun Yat-Sen University. The study protocol was reviewed and approved by the Institutional Animal Care and Use Committee of Sun Yat-Sen University.

Synthesis and Characterization of Copolymer

Synthesis of GA-coupled-poly(Ethylene glycol) (GA-PEG-NH2)

The terminal carboxyl group of GA in dichloromethane (DCM) was activated by adding DCC and NHS at a molar ratio of GA: DCC: NHS = 1: 1.5: 1.5. The mixture was stirred for 8 h under nitrogen protection and filtered to remove N, N'-Dicyclohexylurea (DCU) by-products. The filtrate was precipitated in cold diethylether to form GA-NHS. After drying in vacuum, GA-NHS and NH_2-PEG-NH_2 were mixed at a molar ratio of 1:1.2 in CH_2Cl_2. The mixture was stirred under nitrogen protection at room temperature for 24 h. The solution was concentrated in vacuum, and the product (GA-PEG-NH_2) was precipitated in cold diethylether and collected by filtration. The product was further purified by cation exchange with DEAE Sephadex A-25 (Sigma-Aldrich). The amount of GA in GA-PEG-NH_2 was measured by UV–Vis spectrophotometry (PerkinElmer, Co., USA) at $\lambda = 250$ nm using glycyrrhetinic ammonium salt (Jinzhu Pharmaceutical Co., China) as standard.

Synthesis of poly(lactic-co-glycolic acid)-block-poly(L-histidine) (PLGA-PHIS)

PHIS copolymer was dissolved in 5 mL of 10 mM acetic acid followed by adjustment of pH to 6.5 with 0.1 M NaOH. An excess amount of PLGA-NHS, obtained by activation of PLGA-COOH with NHS, was added to the PHis solution at a molar ratio of PHIS: PLGA = 1: 1.2. Coupling reaction was carried out under nitrogen for 48 h at room temperature. The reaction mixture was dialyzed with cellulose ester membranes (Millipore, Co., USA) with a molecular weight cut-off of 7 kDa against deionized water for 72 h to remove unreacted materials. The product PLGA-PHIS-COOH was obtained by lyophilization.

Synthesis of GA-PEG-PHIS-PLGA (GA-PPP) Block Copolymer

GA-PEG-NH_2, PLGA-PHIS-COOH, DCC, and NHS at a molar ratio = 1.2:1:3:3 were added in DCM. The reaction was carried out at room temperature for 48 h under nitrogen. The solvent was partially evaporated, and polymers in the residue solution were precipitated in diethyl ether. The residual was re-dissolved in DCM, and transferred to a dialysis membrane with a molecular weight cut-off of 7 kDa. The mixture was dialyzed against DCM and deionized water for 48 h, respectively. The outer phase was replaced with fresh deionized water every 12 h. The product GA-PPP was obtained by lyophilization.

The ^{1}H nuclear magnetic resonance (^{1}H-NMR) spectra of copolymers were recorded on a Varian Unity-Plus 400 NMR spectrometer (Varian, Inc., USA) in $CDCl_3$ to verify the structures. Fourier transform infrared assay (FTIR) was performed to provide additional evidence for successful synthesis of co-polymers.

Preparation of AGP-loaded Micelles

AGP-loaded micelles were prepared by a modified solvent evaporation method as described (25). GA-PPP copolymers and AGP were dissolved in acetone : DMF (8:2) mixed solvent (10 mg/mL) and dropped into PBS buffer (pH 7.4,with 0.01% D-α-tocopherol polyethylene glycol 1000 succinate as emulsifier) one drop at a time. The mixed solution was stirred violently for 4 h, packed in a dialysis tube with molecular weight cut-off of 7 kDa, and dialyzed in PBS buffer for 4 h to remove organic solvent. A suspension with AGP-loaded micelles was obtained by filtration with a 0.45 μm membrane. Blank micelles were prepared following the aforementioned approach but without adding AGP.

The loading capacity and efficiency of AGP in micelles were determined by Waters e2695 HPLC (Waters Technology, Co., USA) equipped with a reverse phase C_{18} column (250 × 4.6 mm). The mobile phase is acetonitrile/water (40/60, *v*/*v*) at a flow rate of 1.0 mL/min, and the detection wavelength was 225 nm. The micelle samples were dissolved in acetonitrile to remove the polymeric shells before HPLC analysis. The encapsulation efficiency (EE) and loading efficiency (LE) were calculated using the following equations:

$$EE(\%) = \frac{\text{amount of AGP loaded}}{\text{amount of AGP feeding}} \times 100\%$$

$$LE(\%) = \frac{\text{amount of AGP loaded}}{\text{amount of AGP loaded} + \text{polymer}} \times 100\%$$

Characterization of AGP-loaded Micelles

The size and zeta potential of micelles were determined by doing dynamic light scattering (DLS) at 25°C with a Zetasizer

nano-ZSP (Malvern. Co., UK). Transmission electron microscopy (TEM) was performed using a Tecnai G20 TEM (FEI, Co., USA) at operation voltage of 200KV. Atomic force microscopy (AFM) imaging was performed at room temperature and monitored by a NanoScope IIId controller (Veeco Instruments Co., Plainview, NY, USA) operated in tapping mode and equipped with phase-imaging hardware.

pH-triggered Destabilization of Micelles

Acetic acid was added into GA-PPP suspension (1 mg/mL, pH 7.4) to adjust the pH levels to 6.8, 6.4, 5.8, and 5.0. Samples were gently shaken at 100 rpm at 37°C. After 4 h, changes of micelle sizes and zeta potential in response to different pH conditions were examined using DLS at 37°C. Similar experiments were carried out for the pH-insensitive PEG-PLGA (PP) micelles (1 mg/mL) as controls.

pH-triggered AGP Release from Micelles

AGP release from GA-PPP micelles was examined *in vitro* by dialysis in 0.5% Tween 80 solutions at pH 7.4, 6.4, or 5.0. Briefly, 2 mL AGP/GA-PPP micelle suspension was transferred to a dialysis membrane with a molecular weight cut-off of 3.5 kDa and incubated in a 50 mL sealed bottle at 37°C with stirring at 100 rpm. At the scheduled time-points, 1 mL dialysis solution was collected and filtered with a 0.45 μm membrane, followed by adding the same volume of fresh PBS to the dialysis solution. The AGP contents in the filtrates were measured by HPLC as described above. The cumulative release of AGP was plotted against time.

Cellular Uptake and Localization of Micelles

Cell uptake study was carried out using coumarin 6 (6-C) encapsulated micelles and a human Hep3B hepatoma cell line. 6-C loaded GA-PPP micelles were prepared following the same method as making AGP-loaded GA-PPP micelles. 6-C loaded PEG-PHIS-PLGA (PPP) micelles without GA decoration were also prepared as a control for GA-PPP micelles. The human MDA-MB-231 breast cell line was used as a negative control for Hep3B cells. Cells were seeded into 12-well plates at 2×10^5 cells per well, and cultured for 24 h. Cells were treated with 6-C GA-PPP micelles, 6-C PPP micelles, and free 6-C at a concentration equivalent to 0.1 mg/mL of 6-C for 0.5, 1, 2, or 4 h at 37°C. Cells were washed with PBS and lysed with cell lysis buffer (Abcam, Co., UK). The concentrations of 6-C in cell lysates were quantified by fluorimetry after liquid-liquid extraction by DCM. The total protein content was measured by using the Lowry method. Results were expressed as amount of 6-C (μg) per milligram (mg) of cellular protein.

To further evaluate the cellular uptake of micelles, a confocal laser scanning microscopy (CLSM, Zeiss LSM710) was used to directly visualize the intracellular location of micelles (26). Briefly, Hep3B cells at the logarithm phase were seeded on 35 mm glass dishes at a cell density of 2×10^5/mL for 24 h. Cells were incubated with 6-C/GA-PPP micelles, 6-C/PPP micelles, or free 6-C at a concentration equivalent to 10 μg/mL of 6-C at 37°C for 4 h. Culture medium was removed and the dishes were rinsed with PBS (pH = 7.4) for three times. Cells were fixed in 4% paraformaldehyde for 20 min, stained with Hoechst 33342 for nuclei for 10 min, and imaged with a CLSM.

In Vitro Cell Proliferation and Cell Apoptosis Assays

The cytotoxicity of AGP/GA-PPP micelles was determined using Hep3B cells. AGP loaded in the non-functional PP micelles and free AGP were used as controls. Cells were seeded into 96-well plates at 5000 cells per well and cultured in 100 μL DMEM medium. After incubation for 24 h, culture medium was replaced with 100 μL of fresh medium at pH 7.4 or 6.4 containing free AGP, AGP/PP micelles, or AGP/GA-PPP micelles at different AGP concentrations (0.78 ~ 25 μM). After incubation for 24 h at 37°C, cells were washed and incubated with the MTT dye (5 mg/mL) for 4 h to form formazan crystals. 100 μL of DMSO was added to each well. After gentle shaking for 30 s, cell viability was determined based on the absorbance at 570 nm. Cells not treated with AGP or AGP micelles were used as negative controls. The cytotoxicity of AGP/GA-PPP micelles against L02 cells was also implemented as above-mentioned approach.

The pro-apoptosis effects of AGP loaded micelles and free AGP at a concentration equivalent to 15 μM AGP were determined by the Annexin V/PI staining assay (27). After treatment for 24 h, both non-adherent and adherent cells were collected, washed with cold PBS, and re-suspended in 200 μL binding buffer containing 5 μL Annexin V-FITC. Cells were gently mixed and incubated in dark at room temperature for 10 min. Cells were centrifuged and resuspended in 200 μL binding buffer containing 10 μL propidium iodide (PI) solution. Cell apoptosis was analyzed immediately by a FACS flow cytometer (Beckman coulter) (28).

In Vivo Tissue Distribution

The *in vivo* biodistribution of GA-PPP micelles in BALB/c nude mice was determined by tissue imaging and quantitative biodistribution analysis in different organs, as reported (29–31) and with minor modifications. Indocyanine green (ICG), a tricarbocyanine dye that is currently widely used as a diagnostic aid in the clinics and was approved by FDA, was used as a photosensitizer herein. ICG was loaded into the micelles following the same procedures as preparing AGP

micelles. Nude mice were divided into three groups ($n=3$): free ICG, ICG/PP micelles, and ICG/GA-PPP micelles (0.05 mg/kg equivalent amount of ICG). The samples were administrated to mice *via* tail vein injection. At 0.5, 2, 8 and 24 h after a single injection, mice was sacrificed and organs including heart, liver, spleen, lung, and kidney were collected. Organs were excised, rinsed, and wiped before *ex vivo* imaging with the NightOWL II LB 983 system (Berthold Technologies, USA).

After imaging, these organs were weighed, homogenized in DMSO at a volume 20 times of weight, and extracted by ultrasound at room temperature and in dark for 1 h. Samples were centrifuged at 8000×*g* for 5 min. The concentrations of ICG in the supernatants were measured by a fluorospectrophotometer with excitation at 787 nm and emission at 830 nm.

In Vivo Antitumor Effects

The *ex-situ* liver tumor bearing model was established on BALB/c nude mice by HCC cell transplantation as described (32). When the volume of transplanted tumor reached approximately 500 mm^3, animals were randomly divided into four groups: saline control, free AGP, AGP/PP micelles, and AGP/GA-PPP micelles ($n=6$ animals per group). Tumor bearing mice were injected *via* tail vein with 0.2 mL of different drug formulations at a dose equivalent to 20 mg/kg AGP or saline for once every 2 days within an interval of 27 days. During the treatment period, tumor size and body weight were measured. Tumor volume (v) was calculated as $V=(ab^2)/2$, where a and b indicate the width and length of the tumor, respectively. When the treatment ended, mice were sacrificed and their tumor tissues were weighed. Tumor tissues were fixed with 4% paraformaldehyde for 48 h and embedded in paraffin. After deparaffinization, tissue sections were stained with haematoxylin/eosin (H&E) (33). At least five paraffin sections from each animal were examined for histological changes under an optical microscopy (20).

Statistical Analysis

Statistical analysis was performed by One-Way Analysis of Variance (ANOVA) among three or more groups using SPSS 17.0. Difference was significant at $p<0.05$. All experimental data were expressed as mean ± SD.

RESULTS

Synthesis and Characterization of GA-PPP Copolymer

GA-PPP copolymer was prepared *via* a three-step procedure (Scheme 1). In the first step, GA was coupled to the amino terminal of PEG *via* an amidation reaction. The GA-PEG polymer was confirmed by UV–Vis measurement using 250 nm as the detection wavelength (data not shown). Next, PHIS was conjugated to the terminal carboxyl group of PLGA. Finally, copolymer GA-PPP was conjugated using PHIS as the linkage between PEG and PLGA polymers. The GA coupling amount in GA-PPP copolymer was 4.34 ~ 4.97% (*w*/*w*).

The intermediate products from the polymer synthetic processes were identified by ^{1}H-NMR and FT-IR analysis. The synthetic process of GA-PEG and PLGA-PHIS is characterized by ^{1}H-NMR and FT-IR analysis shown in Supplementary Fig S1 and Fig S2. The ^{1}H NMR spectra for the final step to generate GA-PPP copolymer are shown in Fig. 1. The characteristic signal of protons in $CDCl_3$ appeared at about $\delta=7.2$ ppm. The single peak at $\delta=5.61$ ppm (a) and several peaks at $\delta=0.64$–1.37 ppm (b) were attributed to the protons in the olefinic bond (-(C=O)-CH=C-) of GA (34, 35). The peaks at $\delta=3.52$–3.76 ppm (c) and $\delta=3.25$ ppm (d) were attributed to the protons of the glycol unit (-CH_2-CH_2-O-) and the methylene next to the amino group (-CH_2-N-) in the PEG chain (34). The peaks for PLGA-COOH appeared at $\delta=5.18$ ppm (e) for protons of methine in lactide) and $\delta=4.85$ ppm (f) for protons of methylene in the glycolide (36). The high intensity peak at $\delta=1.6$ ppm (-CO-CH(CH_2)-NH_2) (g) indicated the presence of PHIS (37). All these marker signals were found in the ^{1}H NMR spectrum of GA-PPP copolymers. Moreover, the blunt peak at $\delta=2.21$ ppm, resulted from the -NH_2 group of PEG, disappeared in the spectrum of GA-PPP copolymer, indicating a successful amidation reaction between GA-PEG and PLGA-PHIS copolymers. The appearance of these characteristic peaks in the final product indicated successful synthesis of GA-PPP.

The copolymers were further evaluated by FT-IR. The FT-IR spectra of GA-PEG-PHIS-PLGA are shown in Fig. 2. Because functional groups such as hydroxy groups, carboxyl groups, and amino bonds in GA-PEG and PLGA-PHIS have strong absorption, shifts in the chemical groups can be discovered by FT-IR. For the GA-PEG and GA-PPP polymers, the wide band at around 3480 cm^{-1} was attributed to the inter- and intra-molecular hydrogen bonds of -OH in the PEG polymer as well as the stretching vibration of the three -OH in GA (34). The strong peaks at around 2880 cm^{-1} and the narrow peak at 1112 cm^{-1} were assigned to the -CH_2- and C-O groups in the PEG chain (35, 38). In the PLGA-PHIS polymer, the bands at 2942 and 2851 cm^{-1} corresponded to the -C-H stretching vibration of PLGA (39), and the bands for the C=O bond stretching vibration of carboxyl group appeared at 1665 cm^{-1}. In the GA-PPP copolymer, the band at 1636 cm^{-1} belonged to the C=O bond stretching vibration of -$CONH_2$ group, and the band at 1618 cm^{-1} was related to the bending mode of N-H vibration. Again, these results indicate successful synthesis of GA-PPP.

Scheme 1 The synthesis route of GA-PEG-PHIS-PLGA copolymers.

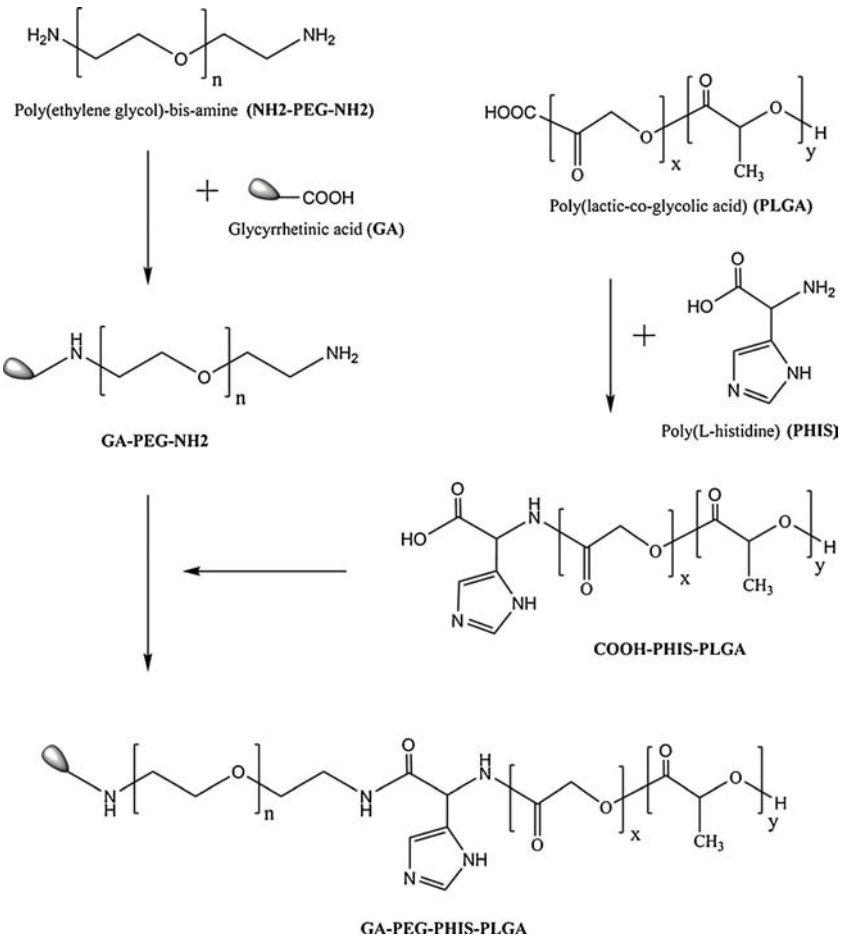

Preparation and Characterization of Micelles

We next prepared drug loaded micelles and evaluated their basic characters. GA-PPP micelles suspension exhibited homogeneous opalescence (Fig. 3a) and the micelles were in a moderate size distribution (Fig. 3b), indicated that micelles may possess EPR properties against tumor tissues. The TEM (Fig. 3c) and AFM (Fig. 3c) images showed that GA-PPP micelles were mono-dispersed and spherically shaped, with no aggregation or adhesion observed, indicating that the suspension was stable. For AGP loaded micelles, the conditions including solvents, polymer weight, and drug amounts

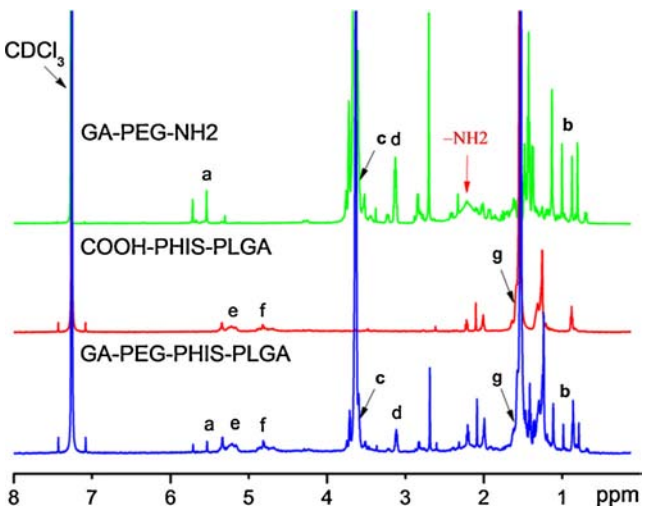

Fig. 1 ^{1}H-NMR spectra of GA-PEG-PHIS-PLGA copolymers.

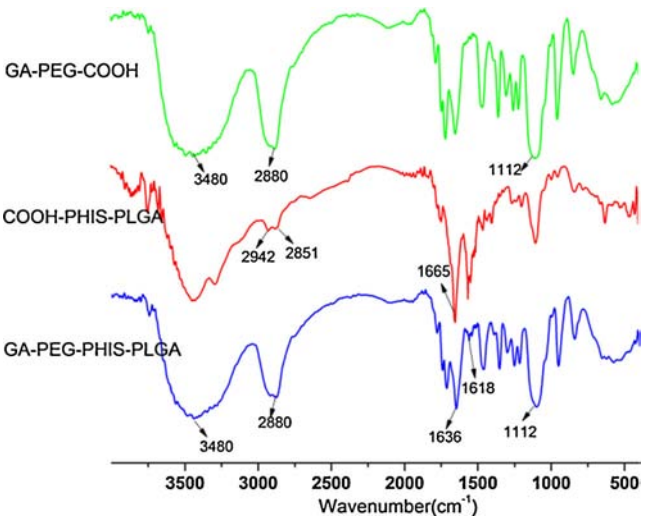

Fig. 2 FTIR spectra of GA-PEG-PHIS-PLGA copolymers.

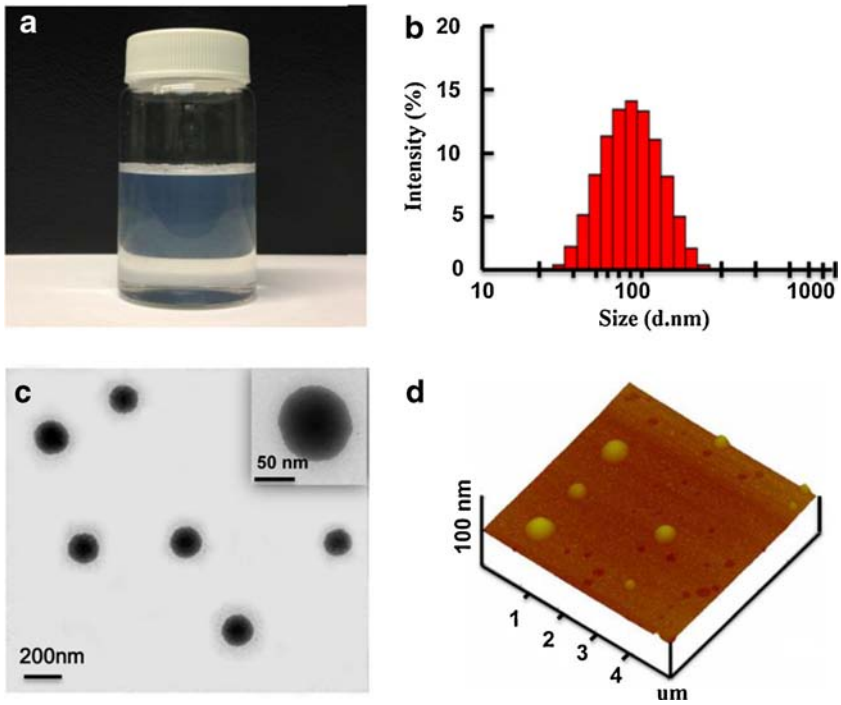

Fig. 3 Characterization of GA-PPP micelles. (**a**) Photographic morphology; (**b**) Size determination by dynamic light scattering (DLS); (**c**) TEM imaging; (**d**) AFM 3D imaging.

were optimized based on the mean diameter (nm), LE (%) and EE (%) of the micelles. The average EE and LE of preparing AGP/GA-PPP micelles in pH 7.4 were 89.6% (*w*/*w*) and 9.1% (*w*/*w*), respectively. Blank PEG-PLGA (PP) micelles and AGP loaded PP (AGP/PP) micelles were prepared as un-functional controls for the subsequent studies. The basic characteristics of these micelles are showed in (Table I). The average size of GA-PPP micelles was larger than that of PP micelles because of the GA-PHIS segment in the GA-PPP copolymer ($^{*}p<0.05$). Compared to blank un-functional PP micelles, the absolute value of zeta potential in the blank GA-PPP micelles was significantly larger($^{\#}p<0.05$), which implied that GA modified micelles had more negative surface charges due to the hydroxyl groups in GA. This negative surface charge kept the micelles stable and away from recognition by hemoglobin *in vivo* (40). Both size and zeta potential of AGP loaded GA-PPP were larger those of AGP loaded PP micelles as well.

pH-responsive Behaviors of GA-PPP Micelles

Tumor cells have early endosomes at pH 6.5 and late endosomes and lysosomes at pH 5.0–6.0 (41). Therefore, five pH levels at 7.4, 6.8, 6.4, 5.8, and 5 were used to mimic the acidic microenvironment in tumors and evaluate the pH-sensitive behavior of GA-PPP micelles. As shown in Fig. 4a, with decreasing pH, sizes of GA-PPP micelles increased accordingly, indicating that the micelles disintegrated in the acidic buffers. Micelles were unstable at pH 6.4 with an average size of 323 nm. At pH 5.8, the shell-core structure of micelles began to collapse as the average size increased to 469 nm. Meanwhile, the zeta potential of micelles rose as pH increased. The turning of zeta potential from negative to positive values indicated protonation of the imidazole of PHIS in acidic buffers. When pH decreased to approximately 6, the imidazole of PHIS became partially protonated and the hydrophilicity of the polymer increased. The increase of hydrophilicity resulted in the destruction of the micelle structures, because the break of hydrophobic crosslinking interlayer lead to micelles burst and drug leaks. Additionally, the increase of zeta potential lead to agglomeration of micelles, as precipitates appeared in the suspension as pH dropped below 6.

To examine AGP release from micelles at different pH conditions, three buffers at pH 7.4, 6.4, and 5 were used as release medium. The drug release profiles were highly pH-dependent. As shown in Fig. 4b, AGP/GA-PPP micelles had limited drug release at pH 7.4, with less than 20% of total drugs accumulated in the medium after 72 h. However, the release rates were significantly increased at pH 6.4 and 5.0. Within 72 h, the total releases of AGP at 6.4 and 5.0 were about 36 and 70%, respectively. These results demonstrated that AGP/GA-PPP micelles were stable at normal physiological pH (7.4) and started to release drugs fast in acidic microenvironment. This character of GA-PPP micelles is useful to reduce release of chemotherapeutic agents from micelles in normal tissue, and accelerate drug release in acidic HCC cells, achieving HCC-targeting drug delivery.

Table I The Basic Characteristics of Blank or AGP-loaded GA-PPP Micelles and PP Micelles as Un-functionalized Controls

Sample	Diameter (nm)	PDI	Zeta Potential (mV)	LE (%)	EE (%)
Blank GA-PPP micelles [a]	92.14 ± 2.56	0.121 ± 0.02	−18.34 ± 2.21		
AGP loaded GA-PPP micelles [a]	126.47 ± 3.74	0.134 ± 0.04	−14.72 ± 2.47	9.1	89.6
Blank unfunctionalized micelles [b]	58.42 ± 1.37	0.105 ± 0.01	−3.43 ± 0.72		
AGP loaded unfunctionalized micelles [b]	84.26 ± 1.96	0.157 ± 0.02	−4.83 ± 0.56	9.6	93.8

[a]: micelles obtained from GA-decorated PEG-PHIS-PLGA copolymers

[b]: micelles obtained from PEG-PLGA copolymers

Hepatoma-targeting Cellular Uptake of Micelles Guided by GA

To evaluate the targetability of GA-PPP micelles to hepatoma cells, 6-C loaded GA-PPP micelles (6-C/GA-PPP) were added to the medium of Hep3B cell, and cellular 6-C levels were measured after incubation for 0.5 to 4 h. For this study, human MDA-MB-231 breast cancer cells were used as a cell line control, and free 6-C and 6-C loaded PPP micelles (6-C/PPP) micelles were used as formulation controls. The uptakes of 6-C in free 6-C solution and 6-C loaded micelles suspensions exhibited a time-dependent manner in MDA-MB-231 (Fig. 5a) and Hep3B cells (Fig. 5b). In both cell lines, their uptakes of 6-C micelles were significantly higher than those of free 6-C ($p<0.05$). There was no significant difference in cellular uptakes between 6-C/GA-PPP and 6-C/PPP micelles in MDA-MB-231 cells (Fig. 5a). However, the uptake of 6-C/GA-PPP micelles was significantly higher than that of 6-C/PPP micelles in Hep3B cells at the 1, 2, 4 h time-points

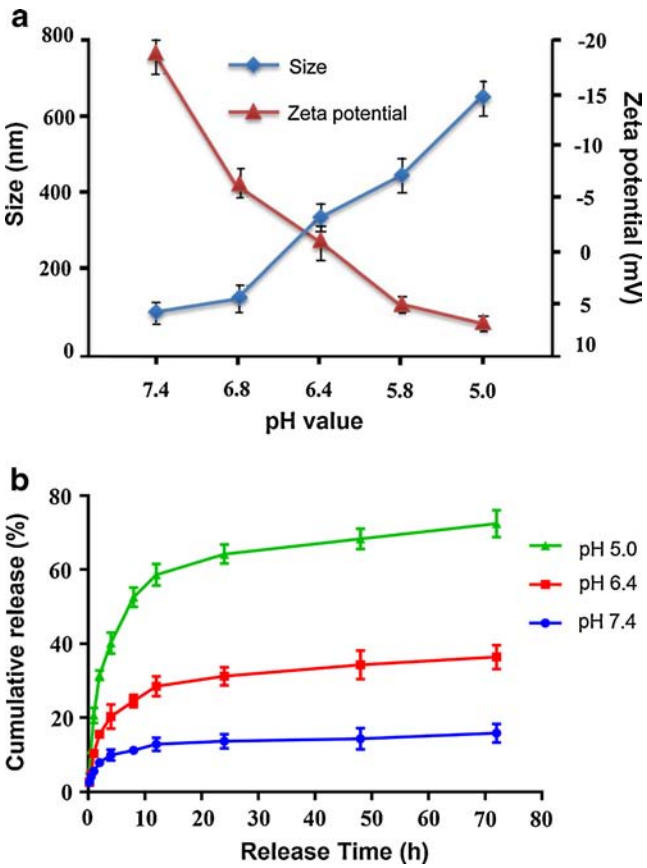

Fig. 4 pH responsive properties analysis of GA-PPP micelles.(**a**) pH-dependent manner of size distribution and zeta potential;(**b**) *in vitro* drug release behavior at different pH conditions.

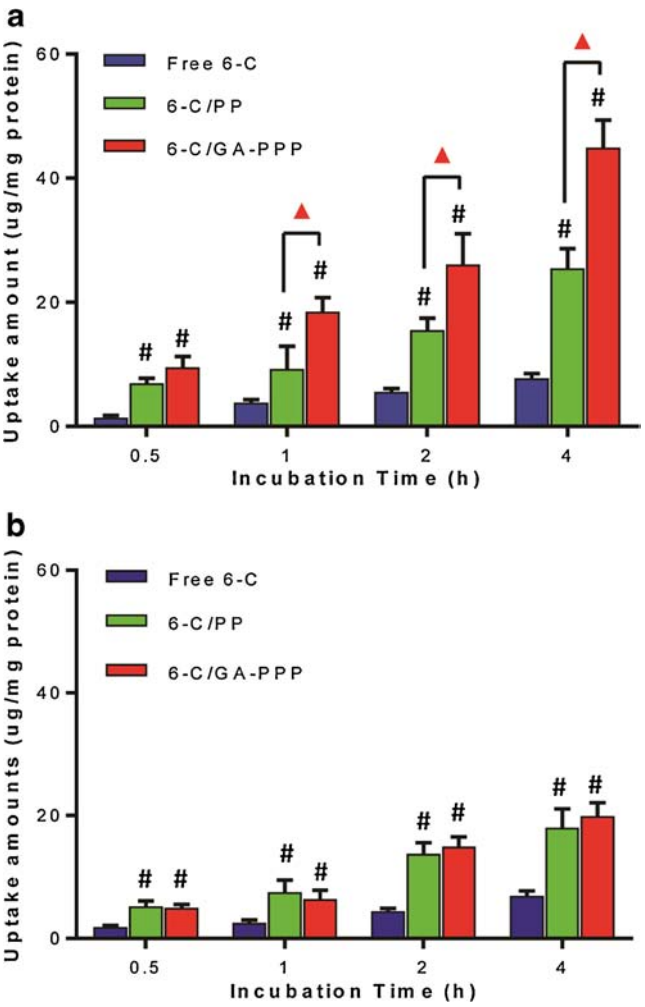

Fig. 5 Uptake of free 6-C and 6-C loaded in micelles in Hep3B cells (**a**) and MDA-MB-231 cells (**b**) at different incubation time with 10 μg/mL amount of 6-C ($n=3$, mean ± SD). ($^{\#}p<0.05$ *VS* free 6-C; $^{\blacktriangle}p<0.05$ denote statistically significant differences between the shown pairs).

($p<0.05$). These results indicated that GA modification increases the affinity of micelles to liver cancer cells and enhances the selective uptake of micelles by HCC cells.

To visualize the cellular internalization of 6-C, Hep3B cells treated with free 6-C or 6-C loaded micelles were observed under a CLSM. As shown in Fig. 6, after incubation with free 6-C or 6-C/PPP for 4 h, weak green fluorescence was observed in the cytoplasm of Hep3B cells. In contrast, after treatment with 6-C/GA-PPP for 4 h, strong intracellular fluorescence was observed in the cytoplasm and nuclei of Hep3B cells. Therefore, GA-PPP micelles are an effective vehicle to rapidly and selectively deliver drugs into hepatoma cells. These results demonstrated that GA modification enhances internalization of micelles to hepatoma cells and improves the affinity of micelles to hepatoma cells.

In Vitro Cell Cytotoxicity

The cytotoxicity of AGP loaded micelles on Hep3B cells was evaluated using the MTT assay (Fig. 7a). Because acidic extracellular environment negatively affects cell growth, we used micelles suspensions at pH 7.4 or 6.4. The drug carriers, blank GA-PPP micelles and PP micelles, did not alter cell viability (Supplementary Fig S3), indicating that blank micelles do not have cytotoxicity against Hep3B cells. After incubation with cells for 24 h, AGP/GA-PPP and AGP/PP micelles had higher cytotoxicity than free AGP at pH 7.4 ($n=3$). At pH 7.4, the IC_{50} values were 27.6 μM for free AGP, 13.5 μM for AGP/PP micelles, and 6.12 μM for AGP/GA-PPP micelles, respectively.

Otherwise, AGP/GA-PPP micelles exhibited significantly higher cytotoxicity at pH 6.4 than at pH 7.4. IC_{50} values of both free AGP and AGP/PP micelles at pH 6.4 were similar as them at pH 7.4, while IC_{50} of AGP/GA-PPP micelles dramatically declined to 3.57 μM. Nevertheless, AGP/GA-PPP micelles at pH 6.4 represented higher cytotoxicity than that at pH 7.4 ($p<0.05$), which was contributed to pH-sensitive drug release of AGP/GA-PPP micelles. Interestingly, non-remarkable cytotoxicity against L02 cells of either free AGP or AGP micelles have been observed (Supplementary Fig S4), indicating its low potential to result in side-effects.

Next, effects of AGP micelles on cell apoptosis, another prominent anticancer mechanism, were analyzed by a flow cytometer after Annexin V-FITC/PI staining. Hep3B cells were treated with free AGP, AGP/PP, or AGP/GA-PPP at a concentration equivalent to 15 μM AGP. Apoptotic rates are shown in Fig. 7b. As

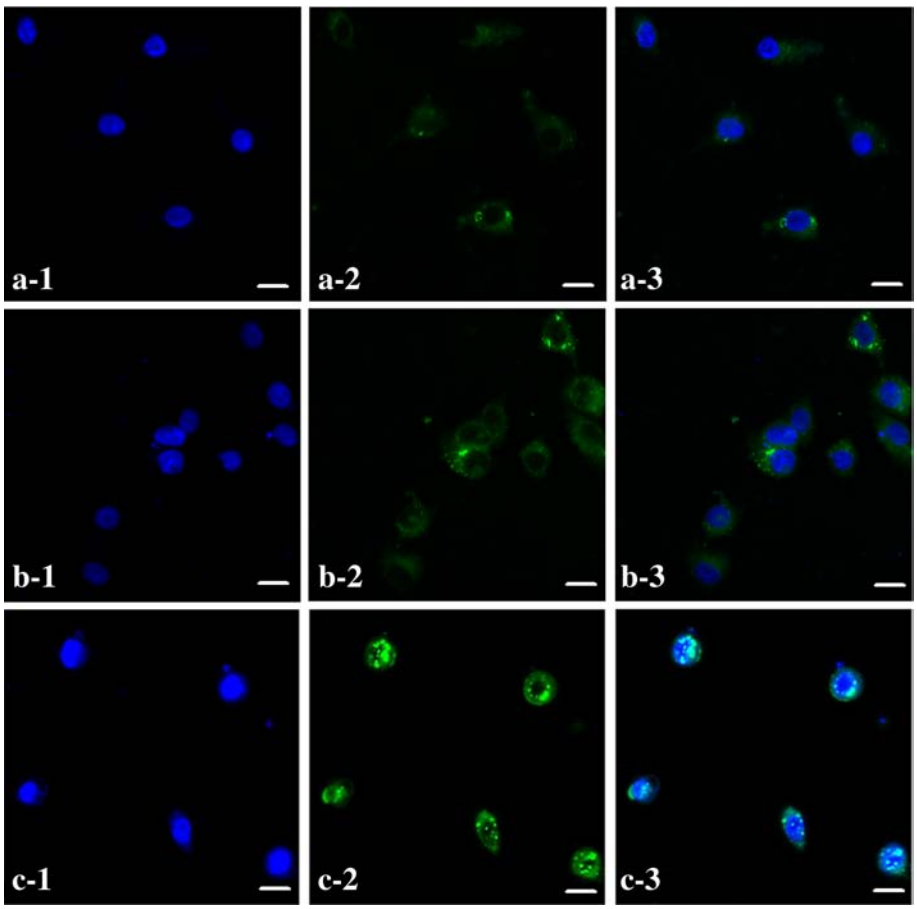

Fig. 6 Cellular internalization imaging of free 6-C (**a**), 6-C loaded PPP micelles (**b**) and 6-C loaded GA-PPP micelles (**c**) with 10 μg/mL amount of 6-C in Hep3B cells following 4 h co-incubation. For each panel, the images from left to right show cell nuclei stained by Hoechst 33342 (blue, 1), 6-C fluorescence in cells (green, 2) and overlays of the two images (3). The scale bars correspond to 20 μm in all the images.

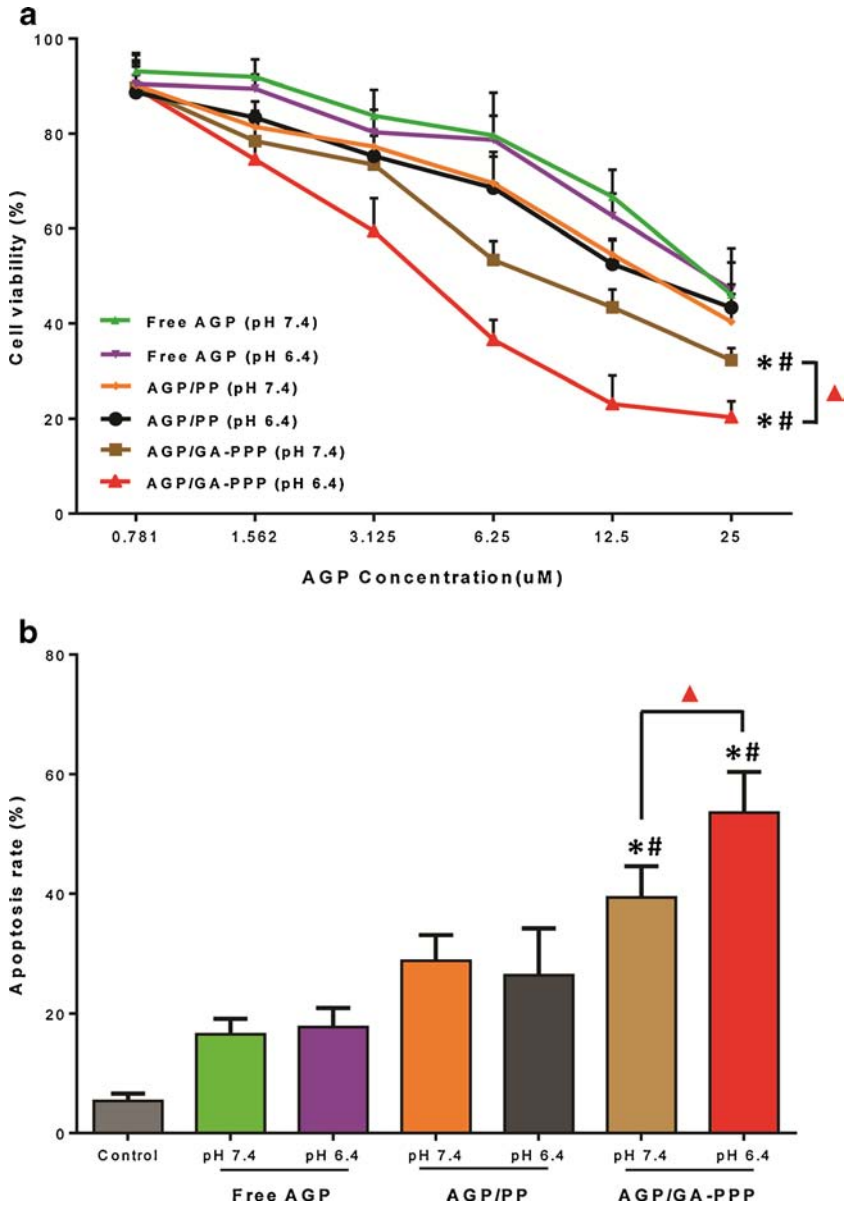

Fig. 7 (**a**) Cytotoxicity results of free AGP and AGP loaded micelles against Hep 3B cells at a series of drug concentration; (**b**) Apoptosis efficacy of free AGP and AGP loaded micelles with 15 μM concentration of AGP. ($^{*}p < 0.05$ *VS* free AGP at pH 6.4; $^{\#}p < 0.05$ *VS* AGP/PP micelles at pH 6.4; $^{\blacktriangle}p < 0.05$ denote statistically significant differences between the shown pairs).

expected, AGP/GA-PPP micelles at pH 6.4 exhibited stronger apoptotic effect than that observed after AGP/GA-PPP micelles treatment at pH 7.4, which opposites to the non-significant differences on cell apoptosis between AGP/PP treatments at pH 6.4 and 7.4. At pH 6.4, the apoptotic rate of AGP/GA-PPP micelles was 1.1- and 2-fold higher compared to the rates of AGP/PP and free AGP treatments, respectively. The pro-apoptosis action of AGP/GA-PPP micelles at pH 6.4 was greatly higher than that of AGP/PP micelles at pH 6.4 and AGP/GA-PPP micelles at pH 7.4 ($p < 0.05$). These results indicated that AGP/GA-PPP micelles are more potent than free AGP against hepatoma cells and that its inhibitory activity is pH-sensitive.

In Vivo Tissue Distribution of Micelles

To examine the cell-targeting effects of GA *in vivo*, we investigated the bio-distribution of ICG loaded micelles with or without GA decoration in mice. Mice were injected with free ICG, ICG/GA-PPP, or ICG/PP. After drug administration for 0.5 h (Fig. 8a), 2 h (Fig. 8b), 8 h (Fig. 8c), and 24 h (Fig. 8d) respectively, mice were sacrificed and their organs including liver, heart, spleen, lung, and kidney were harvested and imaged *in vivo* for their fluorescence. As demonstrated in Fig. 8, encapsulation of ICG in PP (Fig. 8 a-d 1) and GA-PPP (Fig. 8 a-d 2) micelles prolonged the half-life of ICG, with strong fluorescence observed primarily in the liver. However, free ICG was eliminated rapidly in various organs (Fig. 8 a-d 3).

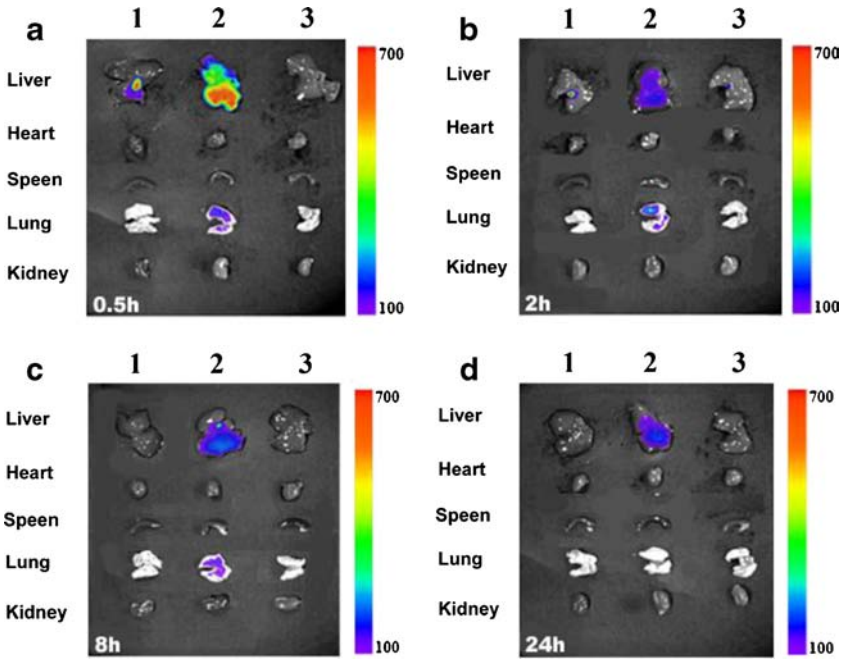

Fig. 8 Fluorescent images in mice harvested organs at 0.5 h (**a**), 2 h (**b**), 8 h (**c**), and 24 h (**d**) post-injection of ICG/PP micelles (1), ICG/GA-PPP micelles(2), and free ICG in saline (3).

Therefore, the chance of false positive of ICG accumulation is very small. Compared to ICG/PP micelles, ICG/GA-PPP micelles were accumulated higher in the liver and retained much longer, with strong fluorescence detected in 24 h after injection.

After *in vivo* imaging, the tissues were homogenized and measured for ICG accumulation (Fig. 9). In consistent with the *in vivo* imaging results, free ICG was eliminated rapidly *via* kidney. In contrast, ICG loaded micelles were accumulated in the lung and liver. The retention time of ICG loaded micelles *in vivo* was significantly prolonged than that of free ICG. In particular, ICG/GA-PPP micelles exhibited significantly higher accumulation in the liver than in any other organs. At each time-point, hepatic accumulation of ICG/GA-PPP micelles was significantly higher than that of ICG/PP micelles or free ICG. These results provided further evidence that GA-modified micelles have higher retention time *in vivo* and exhibit liver-targeting property.

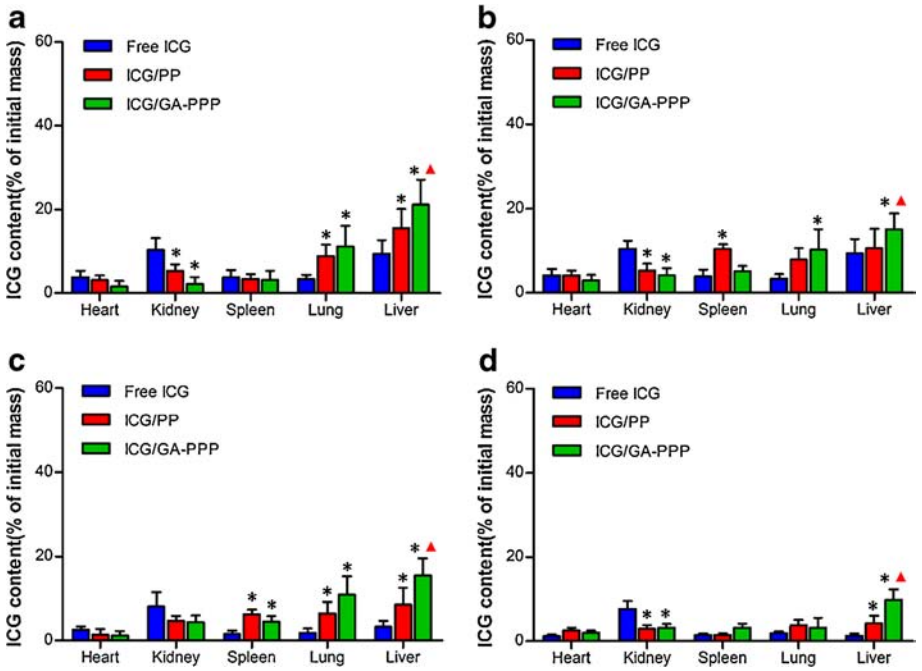

Fig. 9 Distribution of ICG in mice organs after a single intravenous administration of free ICG and ICG loaded micelles at 0.5 h (**a**), 2 h (**b**), 8 h (**c**), and 24 h (**d**).(* $p < 0.05$ *VS* free ICG; ▲$p < 0.05$ *VS* ICG/PP micelles).

In Vivo Anticancer Activity

We next examined the anticancer activity of AGP loaded micelles *in vivo*. After drug administration to BALB/c nude mice bearing *ex-situ* liver tumors for 27 days, the inhibition effects of micelles on tumor volume, tumor weight, and body weight were examined. As seen in Fig. 10a and b, the saline group exhibited a rapid increase in the tumor volume and weight throughout the treatment period. Compared to the saline group, non-significant inhibition of tumor growth was observed in mice after administration of free AGP or AGP/PP micelles. Notably, significant decreases in tumor volume and weight were observed in the group treated with AGP/GA-PPP micelles ($p<0.05$). Because of tumor grafting, the mice received saline injections experienced an approximately 25% decrease of body weight during the treatment period, mainly because of poor appetite (Fig. 10c). However, mice received AGP/GA-PPP micelles maintained their body weight, indicating beneficial effects of AGP/GA-PPP treatment. Representative tumor tissues from different treatment groups are shown in Fig. 10d, in which the antitumor effect of AGP/GA-PPP micelles was the most apparent. The histological results demonstrated the excellent therapeutic effect of AGP/GA-PPP micelles. Representative figures of H&E staining of the tumor tissues treated with different drug formulations are shown in Fig. 10e. Cell apoptosis was observed in the AGP-treated HCC slices. According to the quantitative pathological standard (42), cell apoptosis and tissue necrosis were more severe in the AGP/GA-PPP group than those in the free AGP and AGP/PP groups. Collectively, these results demonstrated that AGP/GA-PPP micelles have great therapeutic effects against Hep3B liver tumor *in vivo*, and the results of AGP/GA-PPP micelles cytotoxicity *in vitro* were able to be extrapolated to *in vivo* results.

DISCUSSION

Enhanced tumor cell uptake, specific tumor accumulation *in vivo* and fast intracellular drug release have been identified as the most common challenges for biodegradable micelles as anticancer drug carriers in clinical translation. To combine active targeting and efficient stimuli-responsive strategies in nano-particular systems has been a promising way. AGP is a bioactive drug isolated from natural plants with anticancer effects on various types of solid malignant tumors and low toxicity. However, its poor bioavailability by fast clearance and poor anticancer efficiency compared to chemotherapeutic agent like Doxorubicin and Sorafenib limits its clinical applications. Therefore, to design a dual-functional nano-micellar system of AGP for HCC treatment is great of interest.

In present study, AGP was encapsulated in GA decorated pH sensitive micelles by solvent evaporation method with narrow particle size distribution, homogeneous spherical structure, monodispersity and optimal EE (Table I). The size of the AGP/GA-PPP micelles was about 120 nm, reaching the requirement of particle size between 70 and 200 nm for cancer treatment (43). The zeta potential of AGP/GA-PPP micelle was around -14 mV, which was beneficial for the colloidal stability in the aqueous solution. With the amphipathic constitute of PEG-PHIS-PLGA copolymer, about 90% amount of AGP could be loaded in the core of micelles. Such high encapsulation efficiency is an outstanding advantage to develop micellar systems instead of conventional nanoparticles such as liposome and microspheres.

Besides the protonation effect of PHIS resulted from the unsaturated nitrogen in imidazole ring, the fusogenicity of PHIS could disrupt the enveloped membrane of acidic subcellular compartments such as endosomes additionally. In that way, PHIS-based micelles have act as promising pH-triggered drug carriers for tumor treatment (37, 44). However, PHIS is too labile to environmental pH, leading to un-stability. In present study, PHIS was set as the linkage polymer between PEG and PLGA, in order to release loaded AGP in tumor fast. According to pH-triggered size change and drug release study, the structure of the micelles was greatly stable (Fig. 4a) and only a small amount of drugs was released (Fig. 4b) at pH 7.4. When pH dropped to 5.0, which was similar as the pH value in endosome, PHIS layer in the micelles became almost protonated and translated to hydrophilicity, so that PHIS blocks could not hold inside the core. The shell-core structure of micelles dissociated, leading up to loaded drug release. Thus, in endosome or lysosome ($pH<6.5$), GA-PPP micelles could react on pH-labile characters by destabilizing and releasing AGP inside tumor cells.

In clinic, many anti-HCC drugs could not reach ideal therapeutic outcome due to the extensive first pass effect and uptake by other cell-types in liver like Kupffer cells, leading to such compounds degradation and therapeutic activity destroyed (45). Thus, in our study, GA was used to modify on surface of micellar systems as the liver targeting ligand to accumulate drugs in hepatocytes. Previous studies revealed micelles decorated by GA could be recognized by GA receptor on hepatocytes to promote drugs uptake and higher accumulation in hepatocytes (46). Conversely, micelles without GA's decoration could not be recognized specifically by liver and accumulated in the liver *via* nonspecific binding and uptake by RES effect only (47). According to the hepatocyte-targeting cellular uptake *in vitro* (Figs. 5 and 6), more fluorescence was detected and observed in cytoplasm of Hep3B cells after incubation of 6-C labeled GA-decorated micelles. It could be concluded that the GA-decorated micelles had a high affinity to Hep3B cells than non-GA-decorated did. Stronger fluorescence of 6-C in cell nucleus also revealed that the induction of GA would benefit the intracellular delivery, resulting in high concentration of drugs loaded in GA-

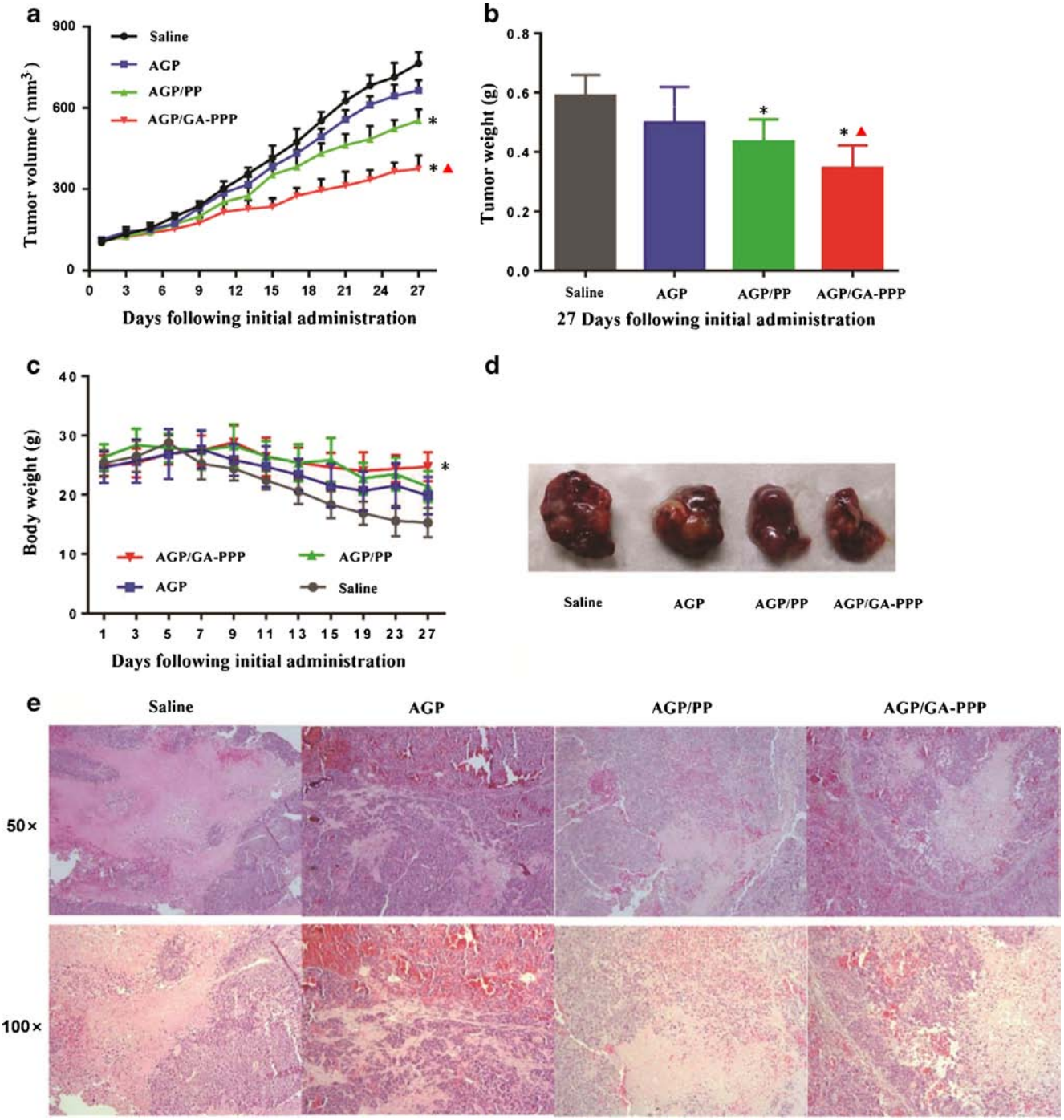

Fig. 10 *In vivo* anticancer activity of AGP/GA-PPP micelles. (**a**) The tumor volume growth of xenografts in all groups; (**b**) The tumor weight of mice in all groups after last administration; (**c**) The body weight of mice in all groups during the treatment period; (**d**) Representative tumor tissues in all groups after treatment; (**e**) Representative images of tumor tissue after last treatment by H&E staining for histopathological analysis. (* $p < 0.05$ *VS* saline control; ▲$p < 0.05$ *VS* AGP/PP micelles)

decorated micelles. Because of the presence of abundant GA receptors on hepatocyte membranes (48), Figs. 8 and 9 results showed GA-modified micelles could target to hepatocytes specifically and keep longer retention period in liver. Although more fluorescence and ICG amounts of ICG-loaded micelles were observed in lung, it did not imply the lung targeting, instead of the filtration in the lung capillary bed (49).

To maintain better anticancer effects after encapsulation is the prerequisite to develop drug delivery system. Both the enhance tumor uptake and pH-labile drug release in tumor provide a synergistic effect on anti-HCC. The cytotoxicity (Fig. 7a) and pro-apoptosis effect (Fig. 7b) against Hep3B cells was followed as: AGP/GA-PPP micelles (pH 6.4) > AGP/GA-PPP micelles (pH 7.4) > AGP/PP micelles (pH 7.4) ≈ AGP/PP

micelles (pH 6.4)>free AGP. The higher cytotoxicity of AGP/GA-PPP micelles than non-GA functional micelles was ascribed to GA receptor mediated endocytosis. AGP/GA-PPP micelles should possess higher cellular uptake in Hep3B cells than AGP/PP micelles. As to the higher cytotoxicity of AGP/GA-PPP at pH 6.4 compared to that at pH 7.4, the acid-triggered release was contributed to it. When AGP/GA-PPP micelles were pre-added in culture medium of pH 6.4 in response to tumor pHe, micelles became loose. Following by endocytosis in cells, AGP loaded was easier and faster to escape from endosome compared to micelles placed in culture medium of pH 7.4.

Furthermore, the antitumor efficiency on tumor bearing mice of AGP/ GA-PPP micelles exhibited stronger than that of free AGP and AGP loaded in non-functional micelles. Both tumor volume and weight in AGP/GA-PPP group were smaller than those in other treated groups. Additionally, body weight was monitored as a marker of overall toxicity. Compared to the greatly reduced body weight in other treated groups, the body weight of AGP/GA-PPP group basically kept stable, indicating these dual-functional micelles presented less toxicity to mice. These significant anticancer effects can be explained as the fast drug release and its efficient endosomal escape by targeting pH-sensitive micelles.

CONCLUSION

In summary, we developed a novel drug delivery system with hepatoma-targeting and pH-responsive properties. In this system, GA was employed as the novel hepatoma-targeting guide, and PHIS acted as the pH-responsive trigger. The dual-functional micelles, *i.e.,* GA-PPP, keep stable in solution at pH 7.4 with desirable particle size and inerratic spherical shape. They become unstable and rapidly release drugs in acidic cellular microenvironment present in the endosomes or lysosomes. Compared to non-GA modified micelles, GA-decorated micelles significantly increased the binding affinity and accumulation in hepatoma cells *in vitro* and in hepatoma tissues *in vivo*. When GA-PPP was loaded with a model anticancer drug AGP, the *in vitro* cytotoxicity and *in vivo* antitumor activity were enhanced remarkably. This study provided a promising strategy to improve targeted therapeutic drug delivery into HCC tumor tissues.

ACKNOWLEDGMENTS AND DISCLOSURES

This study was supported by the Macao Science and Technology Development Fund (062/2013/A2), and the Research Fund of the University of Macau (MRG004/CMW/2014/ICMS, MYRG 208 (Y3-L4)-ICMS11-WYT, MYRG2014-00051-ICMS-QRCM, MYRG2014-00033-ICMS-QRCM), and the fund from National Natural Science Foundation of China (81403120, 21101080).

The authors declare no competing financial interest.

REFERENCES

1. German RR, Fink AK, Heron M, Stewart SL, Johnson CJ, Finch JL, *et al.* The accuracy of cancer mortality statistics based on death certificates in the United States. Cancer Epidemiol. 2011;35(2):126–31.
2. Poelstra K, Prakash J, Beljaars L. Drug targeting to the diseased liver. J Control Release. 2012;161(2):188–97.
3. Gong J, Chen M, Zheng Y, Wang S, Wang Y. Polymeric micelles drug delivery system in oncology. J Control Release. 2012;159(3):312–23.
4. Kedar U, Phutane P, Shidhaye S, Kadam V. Advances in polymeric micelles for drug delivery and tumor targeting. Nanomedicine. 2010;6(6):714–29.
5. Jain RK, Stylianopoulos T. Delivering nanomedicine to solid tumors. Nat Rev Clin Oncol. 2010;7(11):653–64.
6. Zhong Y, Yang W, Sun H, Cheng R, Meng F, Deng C, *et al.* Ligand-directed reduction-sensitive shell-sheddable biodegradable micelles actively deliver doxorubicin into the nuclei of target cancer cells. Biomacromolecules. 2013;14(10):3723–30.
7. Asl MN, Hosseinzadeh H. Review of pharmacological effects of Glycyrrhiza sp. and its bioactive compounds. Phytother Res. 2008;22(6):709–24.
8. Negishi M, Irie A, Nagata N, Ichikawa A. Specific binding of glycyrrhetinic acid to the rat liver membrane. Biochim Biophys Acta. 1991;1066(1):77–82.
9. Tian Q, Zhang CN, Wang XH, Wang W, Huang W, Cha RT, *et al.* Glycyrrhetinic acid-modified chitosan/poly(ethylene glycol) nanoparticles for liver-targeted delivery. Biomaterials. 2010;31(17):4748–56.
10. Tian Q, Wang X, Wang W, Zhang C, Liu Y, Yuan Z. Insight into glycyrrhetinic acid: the role of the hydroxyl group on liver targeting. Int J Pharm. 2010;400(1-2):153–7.
11. Mao SJ, Bi YQ, Jin H, Wei DP, He R, Hou SX. Preparation, characterization and uptake by primary cultured rat hepatocytes of liposomes surface-modified with glycyrrhetinic acid. Pharmazie. 2007;62(8):614–9.
12. Huang W, Wang W, Wang P, Tian Q, Zhang C, Wang C, *et al.* Glycyrrhetinic acid-modified poly(ethylene glycol)-b-poly(gamma-benzyl l-glutamate) micelles for liver targeting therapy. Acta Biomater. 2010;6(10):3927–35.
13. Zhang C, Wang W, Liu T, Wu Y, Guo H, Wang P, *et al.* Doxorubicin-loaded glycyrrhetinic acid-modified alginate nanoparticles for liver tumor chemotherapy. Biomaterials. 2012;33(7):2187–96.
14. Qi WW, Yu H, Guo H, Lou J, Wang Z, Liu P, *et al.* Doxorubicin-loaded Glycyrrhetinic Acid-modified Recombinant Human Serum Albumin Nanoparticles for Targeting Liver Tumor Chemotherapy. Mol Pharm. 2015.
15. Hyodo I, Mizuno M, Yamada G, Tsuji T. Distribution of asialoglycoprotein receptor in human hepatocellular carcinoma. Liver. 1993;13(2):80–5.
16. Gamucci O, Bertero A, Gagliardi M, Bardi G. Biomedical nanoparticles: overview of their surface immune-compatibility. Coatings. 2014;4(1):139–59.
17. Qiu L, Li Z, Qiao M, Long M, Wang M, Zhang X, *et al.* Self-assembled pH-responsive hyaluronic acid–g-poly (l-histidine)

copolymer micelles for targeted intracellular delivery of doxorubicin. Acta Biomater. 2014;10(5):2024–35.
18. Cheng R, Meng F, Deng C, Klok HA, Zhong Z. Dual and multi-stimuli responsive polymeric nanoparticles for programmed site-specific drug delivery. Biomaterials. 2013;34(14):3647–57.
19. Remant Bahadur KC, Thapa B, Xu P. pH and redox dual responsive nanoparticle for nuclear targeted drug delivery. Mol Pharm. 2012;9(9):2719–29.
20. Guo X, Shi C, Wang J, Di S, Zhou S. pH-triggered intracellular release from actively targeting polymer micelles. Biomaterials. 2013.
21. Hu X, Guan X, Li J, Pei Q, Liu M, Xie Z, *et al.* Hybrid polymer micelles capable of cRGD targeting and pH-triggered surface charge conversion for tumor selective accumulation and promoted uptake. Chem Commun (Camb). 2014;50(65):9188–91.
22. Guan XG, Hu XL, Liu S, Huang YB, Jing XB, Xie ZG. Cyclic RGD targeting nanoparticles with pH sensitive polymer-drug conjugates for effective treatment of melanoma. Rsc Adv. 2014;4(98):55187–94.
23. Wang Y, Wang H, Lv X, Liu C, Qi L, Song X, Yu A. Enhancement of All-Trans Retinoic Acid-Induced Differentiation by pH-Sensitive Nanoparticles for Solid Tumor Cells. Macromol Biosci. 2013.
24. Liu Z, Zhang N. pH-Sensitive polymeric micelles for programmable drug and gene delivery. Curr Pharm Des. 2012;18(23):3442–51.
25. Jiang X, Sha X, Xin H, Chen L, Gao X, Wang X, *et al.* Self-aggregated pegylated poly (trimethylene carbonate) nanoparticles decorated with c (RGDyK) peptide for targeted paclitaxel delivery to integrin-rich tumors. Biomaterials. 2011;32(35):9457–69.
26. Zeng X, Tao W, Mei L, Huang L, Tan C, Feng SS. Cholic acid-functionalized nanoparticles of star-shaped PLGA-vitamin E TPGS copolymer for docetaxel delivery to cervical cancer. Biomaterials. 2013.
27. Yuan Y, Liu C, Qian J, Wang J, Zhang Y. Size-mediated cytotoxicity and apoptosis of hydroxyapatite nanoparticles in human hepatoma HepG2 cells. Biomaterials. 2010;31(4):730–40.
28. He YW, Wang HS, Zeng J, Fang XF, Chen HY, Du J, *et al.* Sodium butyrate inhibits interferon-gamma induced indoleamine 2, 3-dioxygenase expression *via* STAT1 in nasopharyngeal carcinoma cells. Life Sci. 2013;93(15):509–15.
29. Ying M, Mostafa S, Jun S. Biodistribution of indocyanine green-loaded nanoparticles with surface modifications of PEG and folic acid. Int J Pharm. 2012;436(1-2):25–31.
30. Zheng C, Zheng M, Gong P, Jia D, Zhang P, Shi B, *et al.* Indocyanine green-loaded biodegradable tumor targeting nanoprobes for *in vitro* and *in vivo* imaging. Biomaterials. 2012;33(22):5603–9.
31. Bahmani B, Lytle CY, Walker AM, Gupta S, Vullev VI, Anvari B. Effects of nanoencapsulation and PEGylation on biodistribution of indocyanine green in healthy mice: quantitative fluorescence imaging and analysis of organs. Int J Nanomedicine. 2013;8:1609–20.
32. Wang Y, Chen H, Liu Y, Wu J, Zhou P, Li R, *et al.* pH-sensitive pullulan-based nanoparticle carrier of methotrexate and combretastatin A4 for the combination therapy against hepatocellular carcinoma. Biomaterials. 2013;34(29):7181–90.
33. Fang X, Dong W, Thornton C, Willett KL. Benzo [a] pyrene effects on glycine N-methyltransferase mRNA expression and enzyme activity in Fundulus heteroclitus embryos. Aquat Toxicol. 2010;98(2):130–8.
34. Wu F, Xu T, Liu C, Chen C, Song X, Zheng Y, He G. Glycyrrhetinic acid-poly (ethylene glycol)-glycyrrhetinic acid triblock conjugates based self-assembled micelles for hepatic targeted delivery of poorly water soluble drug. Sci World J. 2013.
35. Huang W, Wang W, Wang P, Tian Q, Zhang C, Wang C, *et al.* Glycyrrhetinic acid-modified poly (ethylene glycol)–b-poly (γ-benzyl l-glutamate) micelles for liver targeting therapy. Acta Biomater. 2010;6(10):3927–35.
36. Wang JF, Yin C, Tang GP, Lin XF, Wu Q. Synthesis, characterization, and *in vitro* evaluation of two synergistic anticancer drug-containing hepatoma-targeting micelles formed from amphiphilic random copolymer. Biomater Sci-Uk. 2013;1(7):774–82.
37. Wu H, Zhu L, Torchilin VP. pH-sensitive poly (histidine)-PEG/DSPE-PEG co-polymer micelles for cytosolic drug delivery. Biomaterials. 2013;34(4):1213–22.
38. He G, He Z, Zheng X, Li J, Liu C, Song X, *et al.* Synthesis, characterization and *in vitro* evaluation of self-assembled poly (ethylene glycol)-glycyrrhetinic acid conjugates. Lett Org Chem. 2012;9(3):202–10.
39. Stevanović M, Radulović A, Jordović B, Uskoković D. Poly (DL-lactide-co-glycolide) nanospheres for the sustained release of folic acid. J Biomed Nanotechnol. 2008;4(3):349–58.
40. Hartland A, Lead JR, Slaveykova VI, O'Carroll D, Valsami-Jones E. The environmental significance of natural nanoparticles. Nat Educ Knowl. 2013;4(8):7.
41. Yin H, Lee ES, Kim D, Lee KH, Oh KT, Bae YH. Physicochemical characteristics of pH-sensitive poly (l-Histidine)-b-poly (ethylene glycol)/poly (l-Lactide)-b-poly (ethylene glycol) mixed micelles. J Control Release. 2008;126(2):130–8.
42. Shackelford C, Long G, Wolf J, Okerberg C, Herbert R. Qualitative and quantitative analysis of nonneoplastic lesions in toxicology studies. Toxicol Pathol. 2002;30(1):93–6.
43. Gaumet M, Vargas A, Gurny R, Delie F. Nanoparticles for drug delivery: the need for precision in reporting particle size parameters. Eur J Pharm Biopharm. 2008;69(1):1–9.
44. Kim GM, Bae YH, Jo WH. pH-induced Micelle Formation of Poly (histidine-co-phenylalanine)-block-Poly (ethylene glycol) in Aqueous Media. Macromol Biosci. 2005;5(11):1118–24.
45. Smith JS, Xu Z, Byrnes AP. A quantitative assay for measuring clearance of adenovirus vectors by Kupffer cells. J Virol Methods. 2008;147(1):54–60.
46. Tian Q, Wang XH, Wang W, Zhang CN, Wang P, Yuan Z. Self-assembly and liver targeting of sulfated chitosan nanoparticles functionalized with glycyrrhetinic acid. Nanomedicine: Nanotechnol, Biol Med. 2012;8(6):870–9.
47. Banerjee T, Mitra S, Kumar Singh A, Kumar Sharma R, Maitra A. Preparation, characterization and biodistribution of ultrafine chitosan nanoparticles. Int J Pharm. 2002;243(1):93–105.
48. Negishi M, Irie A, Nagata N, Ichikawa A. Specific binding of glycyrrhetinic acid to the rat liver membrane. Biochim Biophys Acta Biomembr. 1991;1066(1):77–82.
49. Zhang L, Yang M, Wang Q, Li Y, Guo R, Jiang X, *et al.* 10-Hydroxycamptothecin loaded nanoparticles: preparation and antitumor activity in mice. J Control Release : Off J Control Release Soc. 2007;119(2):153–62.